

# Rapid immune reconstitution of SCID-X1 canines after G-CSF/AMD3100 mobilization and in vivo gene therapy

Olivier Humbert,<sup>1,\*</sup> Frieda Chan,<sup>1,\*</sup> Yogendra S. Rajawat,<sup>1</sup> Troy R. Torgerson,<sup>2,3</sup> Christopher R. Burtner,<sup>1</sup> Nicholas W. Hubbard,<sup>2,4</sup> Daniel Humphrys,<sup>1</sup> Zachary K. Norgaard,<sup>1</sup> Patricia O'Donnell,<sup>5</sup> Jennifer E. Adair,<sup>1,6</sup> Grant D. Trobridge,<sup>7</sup> Andrew M. Scharenberg,<sup>2,4</sup> Peter J. Felsburg,<sup>5</sup> David J. Rawlings,<sup>2,4</sup> and Hans-Peter Kiem<sup>1,6,8</sup>

<sup>1</sup>Stem Cell and Gene Therapy Program, Fred Hutchinson Cancer Research Center, Seattle, WA; <sup>2</sup>Center for Immunity and Immunotherapies, Seattle Children's Research Institute, Seattle, WA; <sup>3</sup>Department of Pediatrics and <sup>4</sup>Department of Immunology, University of Washington, Seattle, WA; <sup>5</sup>Department of Clinical Studies, School of Veterinary Medicine, University of Pennsylvania, Philadelphia, PA; <sup>6</sup>Department of Medicine, University of Washington School of Medicine, Seattle, WA; <sup>7</sup>Department of Pharmaceutical Sciences, Washington State University, Pullman, WA; and <sup>8</sup>Department of Pathology, University of Washington School of Medicine, Seattle, WA

## Key Points

- IV delivery of FV vector using the phosphoglycerate kinase promoter outperforms EF1 $\alpha$ -containing vector in the canine SCID-X1 model.
- G-CSF/AMD3100 mobilization before in vivo FV vector delivery improves kinetics and clonal diversity of lymphocyte reconstitution.

Hematopoietic stem-cell gene therapy is a promising treatment of X-linked severe combined immunodeficiency disease (SCID-X1), but currently, it requires recipient conditioning, extensive cell manipulation, and sophisticated facilities. With these limitations in mind, we explored a simpler therapeutic approach to SCID-X1 treatment by direct IV administration of foamy virus (FV) vectors in the canine model. FV vectors were used because they have a favorable integration site profile and are resistant to serum inactivation. Here, we show improved efficacy of our in vivo gene therapy platform by mobilization with granulocyte colony-stimulating factor (G-CSF) and AMD3100 before injection of an optimized FV vector incorporating the human phosphoglycerate kinase enhancerless promoter. G-CSF/AMD3100 mobilization before FV vector delivery accelerated kinetics of CD3<sup>+</sup> lymphocyte recovery, promoted thymopoiesis, and increased immune clonal diversity. Gene-corrected T lymphocytes exhibited a normal CD4:CD8 ratio and a broad T-cell receptor repertoire and showed restored  $\gamma$ C-dependent signaling function. Treated animals showed normal primary and secondary antibody responses to bacteriophage immunization and evidence for immunoglobulin class switching. These results demonstrate safety and efficacy of an accessible, portable, and translatable platform with no conditioning regimen for the treatment of SCID-X1 and other genetic diseases.

## Introduction

Human X-linked severe combined immunodeficiency (SCID-X1) is a failure of both cellular and humoral immune responses caused by mutations in the common  $\gamma$  chain gene ( $\gamma$ C), which results in the absence of T and natural killer (NK) cells and dysfunctional B lymphocytes. SCID-X1 is fatal in the first 2 years of life unless the immune system is reconstituted through bone marrow transplantation (BMT) or gene therapy. Because most individuals lack a matched donor, haploidentical parental bone marrow depleted of mature T cells is often used.<sup>1,2</sup> However, this procedure is limited by risks of graft-versus-host disease and incomplete immune reconstitution, resulting in failure to make adequate antibodies and hence requiring long-term immunoglobulin replacement, late loss of T cells because of failure to engraft hematopoietic stem cells, chronic warts, and lymphocyte dysregulation.

An alternative approach to BMT is ex vivo hematopoietic stem and progenitor cell (HSPC) gene therapy, where blood or marrow HSPCs are enriched from patients, transduced with viral vectors to deliver the functional  $\gamma$ C gene, and transplanted back into the patient. Although self-inactivating (SIN)

gammaretroviral vectors (RVs) and SIN lentiviral vectors (LVs) are currently used in the clinical setting with considerable success,<sup>3,4</sup> ex vivo gene therapy still faces multiple challenges that include: (1) the extensive manipulation of HSPCs, resulting in loss of multipotency and/or reduced fitness for engraftment after transplantation, (2) considerable genotoxic risks to the patients of various conditioning regimens used to enhance engraftment of gene-modified HSPCs, and (3) need for advanced infrastructures for the collection, culture, transduction, validation, and reinfusion of HSPCs, consequently restricting this form of treatment to a select few institutions worldwide. With these limitations in mind, we explored in vivo gene therapy, which consists of the direct delivery of the viral vector to the patient. In vivo gene therapy is a simple and attractive approach because it requires neither genotoxic conditioning nor ex vivo cell processing and thus can be adopted at many institutions worldwide, including those in developing countries.

To evaluate these novel therapeutic approaches, we used the canine SCID-X1 preclinical model because it has nearly identical disease phenotype and clinical manifestation when compared with human SCID-X1.<sup>5-7</sup> Both human and canine SCID-X1 are characterized by absent thymic T-cell development and dysregulated B-cell germinal center responses, leading to low immunoglobulin levels (immunoglobulin A [IgA] and IgG), failure to thrive, and early mortality resulting from viral and/or bacterial infection.<sup>8-13</sup> The utility of this model was previously validated by studies employing ex vivo HSPC gene therapy (reviewed by Felsburg et al<sup>14</sup>) and more recently by direct IV administration of the viral vector.<sup>15</sup> Unlike VSV-G pseudotyped LVs, foamy virus (FV) vectors are resistant to human serum inactivation,<sup>16</sup> which gives them a specific advantage during in vivo delivery. FV vectors are nonpathogenic integrating retroviruses,<sup>16-18</sup> which are highly effective for HSPC gene transfer<sup>19-22</sup> and potentially safer than SIN RVs and SIN LVs because of their favorable integration profile.<sup>23,24</sup> These properties contribute to their safety as established in the canine model<sup>21,25,26</sup> and in the murine xenotransplantation model.<sup>20,27-29</sup>

We previously demonstrated the feasibility of in vivo gene therapy in canine SCID-X1 with IV injection of FV vector expressing human codon optimized  $\gamma$ C driven by the short elongation factor-1  $\alpha$  promoter (EF1 $\alpha$ ; EF1 $\alpha$ . $\gamma$ C.FV).<sup>30</sup> Successful lymphocyte expansion was reported in these animals, but clonal diversity and T-cell receptor (TCR) repertoire were low, which prompted further optimization of our method. In the current study, we began by investigating the use of an alternative promoter derived from the human phosphoglycerate kinase (PGK) gene on our FV vector (PGK. $\gamma$ C.FV) and then studied the use of a cell mobilization regimen with granulocyte colony-stimulating factor (G-CSF) and AMD3100 before in vivo FV vector administration. This novel approach substantially improved therapeutic outcome by accelerating kinetics of CD3<sup>+</sup> lymphocyte recovery and increasing thymopoiesis and immune clonal diversity.

## Materials and methods

### Study approval

All experiments were performed in accordance with protocols approved by the University of Pennsylvania and Fred Hutchinson Cancer Research Center Institutional Animal Care and Use Committees (#50855 at Fred Hutchinson).

## Mobilization regimen and FV vector injection

SCID-X1-affected neonatal pups at ~1 kg (age 3 weeks) were injected subcutaneously (SQ) with 5  $\mu$ g/kg of canine G-CSF twice per day for 4 days and with a last single dose of canine G-CSF (5  $\mu$ g/kg SQ) with AMD3100 (4 mg/kg SQ) 6 to 8 hours prior on the day of FV vector injection for mobilization of hematopoietic stem cells (HSCs); this dose regimen was previously published by Thakar et al.<sup>31</sup> Six hours after AMD3100 administration and immediately before FV vector injection, 0.5 mL of peripheral blood was collected to measure CD34<sup>+</sup> cell frequency in peripheral blood by staining with anti-canine CD34 monoclonal antibody (clone 1H6; Serotec, Raleigh, NC). For vector administration, the injection site was sterilely prepared, and a 23-G catheter was placed in the cephalic vein. Vector was administered slowly over 2 to 5 minutes, and animals were monitored for injection-related reactions. If required, antihistamines and anti-inflammatories (glucocorticoids) were administered. Animals were monitored for temperature, pulse, and respiration rates every 15 minutes for next 2 hours and hourly thereafter for the following 24 hours.

## FV vectors

FV vectors were produced by polyethylenimine transfection of 4 plasmids in HEK293T cells as previously described,<sup>32</sup> with the exception that 37.7  $\mu$ g of transfer plasmid and 10.8, 16.1, and 0.8  $\mu$ g of FV helper plasmids pFVGagCO, pFVPolCO, and pFVEnvCO, respectively, and 198.6  $\mu$ L of 1  $\mu$ g/ $\mu$ L polyethylenimine were used per 15-cm plate. The FV helper plasmids were codon optimized to improve expression and to eliminate the potential for recombination. Vector-containing supernatant was passed through a 0.45- $\mu$ m filter, concentrated 100-fold by ultracentrifugation at 23°C, titered on HT1080 cells, and frozen at -80°C until use in Iscove modified Dulbecco medium containing 5% dimethyl sulfoxide.

## Determination of in vivo gene marking and phenotype analysis

Gene marking and phenotype analysis of peripheral blood leukocytes were determined by flow cytometry using antibodies described in our previous study.<sup>30</sup> Surface interleukin-2 (IL-2) receptor  $\gamma$ C expression was determined by staining with APC anti-human CD132 antibody clone TUGh4 (Biolegend, San Diego, CA). Blood was collected in EDTA or heparin tubes, subjected to hemolysis, and washed in phosphate-buffered saline plus 2% fetal bovine serum. Flow cytometry analysis was performed on either a BD LSR II or FACSCanto flow cytometer (Becton Dickinson, San Jose, CA) to measure fluorescent gene marking or fluorescent antibody cell-surface receptor phenotyping. Vector copy number was determined by measuring WPRE levels with the TaqMan quantitative real-time polymerase chain reaction (PCR) assay. 300 ng of genomic peripheral blood leukocyte DNA was amplified at least in duplicate with a WPRE-specific primer/probe combination (5'-CCT CCT TGT ATA AAT CCT GGT TG-3' and 5'-GGT TGC GTC AGC AAA CAC AG-3'; probe: 5'-FAM-GAG GAG TTG TGG CCC GTT GTC-TAMRA-3'). A canine IL-3-specific primer/probe combination (5'-ATG AGC AGC TTC CCC ATC C-3', 5'-GTC GAA AAA GGC CTC CCC-3'; probe: 5'-FAM-TCC TGC TTG GAT GCC AAG TCC CAC-TAMRA-3') was used to adjust for equal loading of genomic DNA (gDNA).

**Table 1. Animals treated with in vivo FV vector gene therapy**

ID	Weight at injection, kg	Age at injection, d	FV	Dose of vector, IU	Mobilization	WBCs, × 10 <sup>9</sup> /L	Estimated MOI*
R2202	NA	1	EF1 $\alpha$ .GFP.2A. $\gamma$ C	4.2 × 10 <sup>8</sup>	No	NA	NA
R2203	NA	1	EF1 $\alpha$ .GFP.2A. $\gamma$ C	4.2 × 10 <sup>8</sup>	No	NA	NA
R2258	1.04	18	EF1 $\alpha$ .GFP.2A. $\gamma$ C	4.0 × 10 <sup>8</sup>	No	7.67	1.21
			PGK.mCherry.2A. $\gamma$ C	4.0 × 10 <sup>8</sup>			
R2260	1.05	18	EF1 $\alpha$ .mCherry.2A. $\gamma$ C	4.0 × 10 <sup>8</sup>	No	6.64	1.40
			PGK.GFP.2A. $\gamma$ C	4.0 × 10 <sup>8</sup>			
H864	0.8	16	PGK.mCherry.2A. $\gamma$ C	4.0 × 10 <sup>8</sup>	G-CSF/ AMD3100	16.42	0.28
H867	1.1	16	PGK.mCherry.2A. $\gamma$ C	4.0 × 10 <sup>8</sup>	G-CSF/ AMD3100	18.04	0.26

IU, infectious units; MOI, multiplicity of infection; NA, not available; WBC, white blood cell.

\*MOI at the time of injection was calculated based on the number of virus particles injected divided by the estimated number of circulating WBCs (considering an average blood volume of 86 mL/kg).

### Foamy RIS analysis

Retrovirus integration site (RIS) analysis was performed as previously described.<sup>33,34</sup> gDNA was extracted from leukocytes collected at various time points from either peripheral blood or bone marrow or from the tissues harvested at necropsy by Qiagen Blood DNA Mini Kit or Gentra Puregene Blood kit (both from Qiagen), per manufacturer instructions. FV vector long terminal repeat–genome junctions were amplified by modified genomic sequencing PCR as described.<sup>30</sup> Resulting sequence libraries were subjected to paired-end Illumina MiSeq platform sequencing. RISs were identified using a bioinformatic method as previously described in detail. Valid integration sites were scored after locating primer sequence, FV long terminal repeats, absence of FV vector sequence, and potential canine gDNA. Potential genomic sequences were mapped to the canine genome (canFam3) using a standalone version of BLAT available from the University of California Santa Cruz Genome Browser. Sequences corresponding to the same genomic locus were grouped together to determine the total number of unique RIS events (clones) identified in the sample. Additional details on bioinformatic analysis of data are given below.

### In vitro T-lymphocyte functional assay

In the mitogen-induced proliferation assay, peripheral blood mononuclear cells (PBMCs) were isolated by ficoll centrifugation, and 1 × 10<sup>6</sup> to 2 × 10<sup>6</sup> cells were stimulated with 5  $\mu$ g/mL of phytohemagglutinin (Sigma, St. Louis, MO) for 48 hours in complete medium at 37°C and 5% carbon dioxide. Cell proliferation was assessed using flow cytometric CellTracker™ dye assay (ThermoFisher Scientific) as per manufacturer instruction. For phosphorylated STAT5 (pSTAT5) and pSTAT3 analysis, PBMCs were incubated for 4 to 6 hours at 37°C and 5% carbon dioxide in complete medium (RPMI with 10% fetal calf serum, 1% L-glutamine, and 0.5% Pen/Strep), after which they were stimulated with IL-2 or IL-21 for 20 to 25 minutes as described previously.<sup>30</sup> pSTAT3 and pSTA5 phosphorylation was subsequently monitored by intracellular staining with pSTAT3 antibody (BD Phosflow cat #557815) and pSTAT5 y694 antibody (BD Phosflow cat #612599), respectively, and analyzed by flow cytometry.

### Bacteriophage immunization assay

Generation of specific antibody responses and immunoglobulin class switching was assessed after immunization with the

T cell–dependent neoantigen bacteriophage  $\phi$ X174. This bacteriophage does not replicate or cause illness in humans and induces helper T cell–dependent antibody response when used as immunogen.<sup>35</sup> Mobilized (H864 and H867) and nonmobilized (R2258 and R2260) animals were injected with a first dose of bacteriophage  $\phi$ X174 at 8 to 12 months post–FV vector treatment and with a second dose 6 weeks later, and immune response was assessed at 1, 2, and 4 weeks postinjection. Total  $\phi$ X-174–specific antibody in each plasma sample was determined by using a standardized phage neutralization assay<sup>36</sup> and was expressed as the rate of phage inactivation or K value as derived from a standard formula. Specific antibody levels were plotted as log K value against time. Total antibody production (pan IgG, IgA, IgM) was quantitatively measured (test code SO633; Phoenix Laboratories, Seattle, WA) from serum collected from FV-treated animals.

### TCR spectratyping and TREC analysis

For spectratyping analysis, peripheral blood was hemolysed and RNA was extracted from 5 × 10<sup>6</sup> white blood cells using the RNeasy Mini Kit (cat #74104; Qiagen, Valencia, CA). Complementary DNA was generated from 100 to 400 ng of RNA using 200 U of SuperScript II Reverse Transcriptase (cat #18064-022; Invitrogen, Grand Island, NY) and oligo dT following manufacturer instructions. Complementary DNA was amplified using 17 specific forward TCR vector  $\beta$  primers and a common 6-FAM–conjugated reverse primer, as previously published.<sup>37</sup> The products were analyzed on an Applied Biosystems ABI 3730xl DNA Analyzer, and GeneMapper software (version 4.0) was used for the analysis of peak sizes (Life Technologies, Grand Island, NY). For TCR excision circle (TREC) analysis, peripheral blood was lysed and DNA was extracted from 5 × 10<sup>6</sup> cells using the Qiagen QIAamp DNA Blood Mini Kit (cat #51106). A real-time quantitative PCR method was used as previously described to detect signal joint TRECs.<sup>38</sup>

## Results

### Improved gene marking and lymphocyte reconstitution in vivo using vector PGK. $\gamma$ C.FV

To optimize our in vivo gene therapy protocol, we began by comparing FV vector using EF1 $\alpha$ . $\gamma$ C.FV with an identical vector containing the PGK promoter (PGK. $\gamma$ C.FV). In vitro transduction of human and canine CD34<sup>+</sup> cells using matching doses of each

vector showed increased expression by approximately twofold in both cell types for PGK. $\gamma$ C.FV, determined by *cis*-linked fluorophore expression as surrogate marker (supplemental Figure 1). EF1 $\alpha$ . $\gamma$ C.FV and PGK. $\gamma$ C.FV were then directly compared *in vivo* using a competitive repopulation assay, in which 2 newborn SCID-X1 animals were injected intravenously with equal doses of each FV vector (R2258 and R2260; Table 1). Distinct *cis*-linked fluorophore, GFP or mCherry (linked to the  $\gamma$ C gene with a T2A peptide), was used to track immune reconstitution, and the configuration of the fluorophores was permuted in the second animal to rule out any effect of the reporter gene. As shown in Figure 1A and Table 1, R2258 was injected with combination of EF1 $\alpha$ .GFP.2A. $\gamma$ C.FV and PGK.mCherry.2A. $\gamma$ C.FV, whereas R2260 was injected with EF1 $\alpha$ .mCherry.2A. $\gamma$ C.FV and PGK.GFP.2A. $\gamma$ C.FV (total of  $4.0 \times 10^8$  infectious units or an estimated multiplicity of infection of 1.21 or 1.40, respectively, at the time of injection).

The absolute number of circulating lymphocytes steadily increased in both treated dogs during the course of 2.5 years posttreatment while remaining within the normal range (Figure 1B). Strikingly, a majority of gene marking (70% to 90%) in peripheral blood came from the PGK. $\gamma$ C.FV vector in both animals, whereas marking from the EF1 $\alpha$ . $\gamma$ C.FV vector comprised only a small fraction (5% to 10%; Figure 1C). Interestingly, the early kinetics of gene marking in peripheral blood lymphocytes in these 2 animals was substantially improved as compared with animals treated with the EF1 $\alpha$ . $\gamma$ C.FV vector in our previous study<sup>30</sup> (R2202 and R2203; Table 1). As shown in Figure 2C, the fraction of gene-corrected peripheral lymphocytes reached 40% in both R2258 and R2260 at 6 weeks postinjection, as compared with <5% for the EF1 $\alpha$ . $\gamma$ C.FV-treated animals<sup>30</sup> (compare blue and orange lines). These results demonstrated superior therapeutic performance of the PGK. $\gamma$ C.FV vector, which will be the preferred vector platform for subsequent experiments using *in vivo* delivery.

### G-CSF/AMD3100 mobilization enhances kinetics of T-lymphocyte expansion and immune clonal diversity in FV-treated animals

Although a majority of circulating T lymphocytes expressed the  $\gamma$ C transgene in treated SCID-X1 dogs, marking in cell lineages with no selective advantage such as B lymphocytes and myeloid cells was low, albeit above background (supplemental Figures 2A-B and 3), suggesting that our delivery approach did not effectively target the most primitive HSCs. Previous studies showed that a combination of G-CSF and AMD3100 efficiently mobilizes multipotent progenitor cells in peripheral blood in animal models and in patients.<sup>39-42</sup> On the basis of these findings, we treated 2 SCID-X1 canine pups at ~3 weeks of age with 5  $\mu$ g/kg of G-CSF twice per day from day -4 to -1 before FV injection and a single dose of G-CSF with 4 mg/kg of AMD3100 on the morning of the injection (animals H864 and H867; Table 1; Figure 2A). Treatment was well tolerated and resulted in a 6.4- to 7.2-fold increase in circulating CD34<sup>+</sup> cells at 6 hours post-AMD3100 administration (2.30% and 2.59% of total white blood cells in the 2 mobilized SCID-X1 animals, respectively, as compared with 0.36% in a nonmobilized littermate normal control, consistent with values for steady state hematopoiesis<sup>9</sup>; Figure 2B).

Injection of vector PGK.mCherry.2A. $\gamma$ C.FV at 6 hours post-AMD3100 administration significantly increased the kinetics

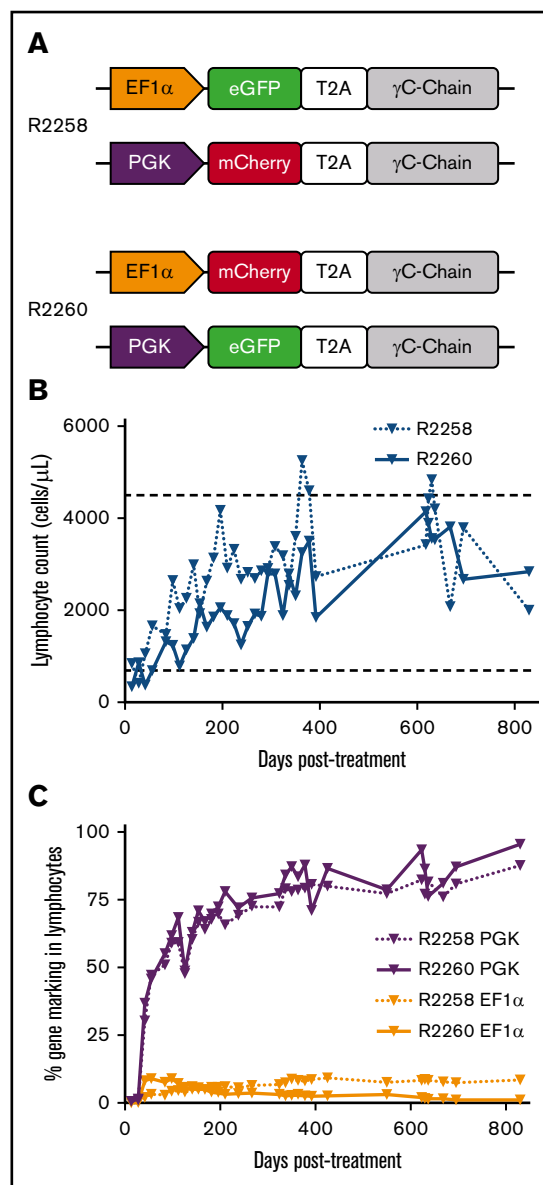


**Figure 1. Competitive injection of SCID-X1 dogs with EF1 $\alpha$  and PGK FV vectors.** (A) Dogs R2258 and R2260 were injected with a combination of FV vectors PGK. $\gamma$ C.FV and EF1 $\alpha$ . $\gamma$ C.FV containing the fluorophores eGFP or mCherry. (B) Kinetics of lymphocyte reconstitution (lymphocytes per microliter of peripheral blood) in R2258 and R2260. Range of lymphocyte counts in healthy dogs is shown by horizontal dashed lines. (C) Long-term analysis of gene marking in peripheral blood lymphocytes from R2258 and R2260 for the PGK and EF1 $\alpha$  FV vectors based on fluorophore expression. Lymphocyte population was defined based on forward and side scatter. T2A, thea asigna virus 2A self-cleaving peptide.

of lymphocyte expansion and gene marking as compared with kinetics in nonmobilized FV-treated animals, despite lower estimated multiplicity of infections at the time of vector injection (0.28 and 0.26; Table 1). The fraction of gene-corrected lymphocytes in peripheral blood of mobilized animals reached 80% at 6 weeks posttreatment, whereas it took >20 weeks in nonmobilized animals to reach similar levels (Figure 2C). Accordingly, the time required to reach normal lymphocyte counts was markedly reduced in the



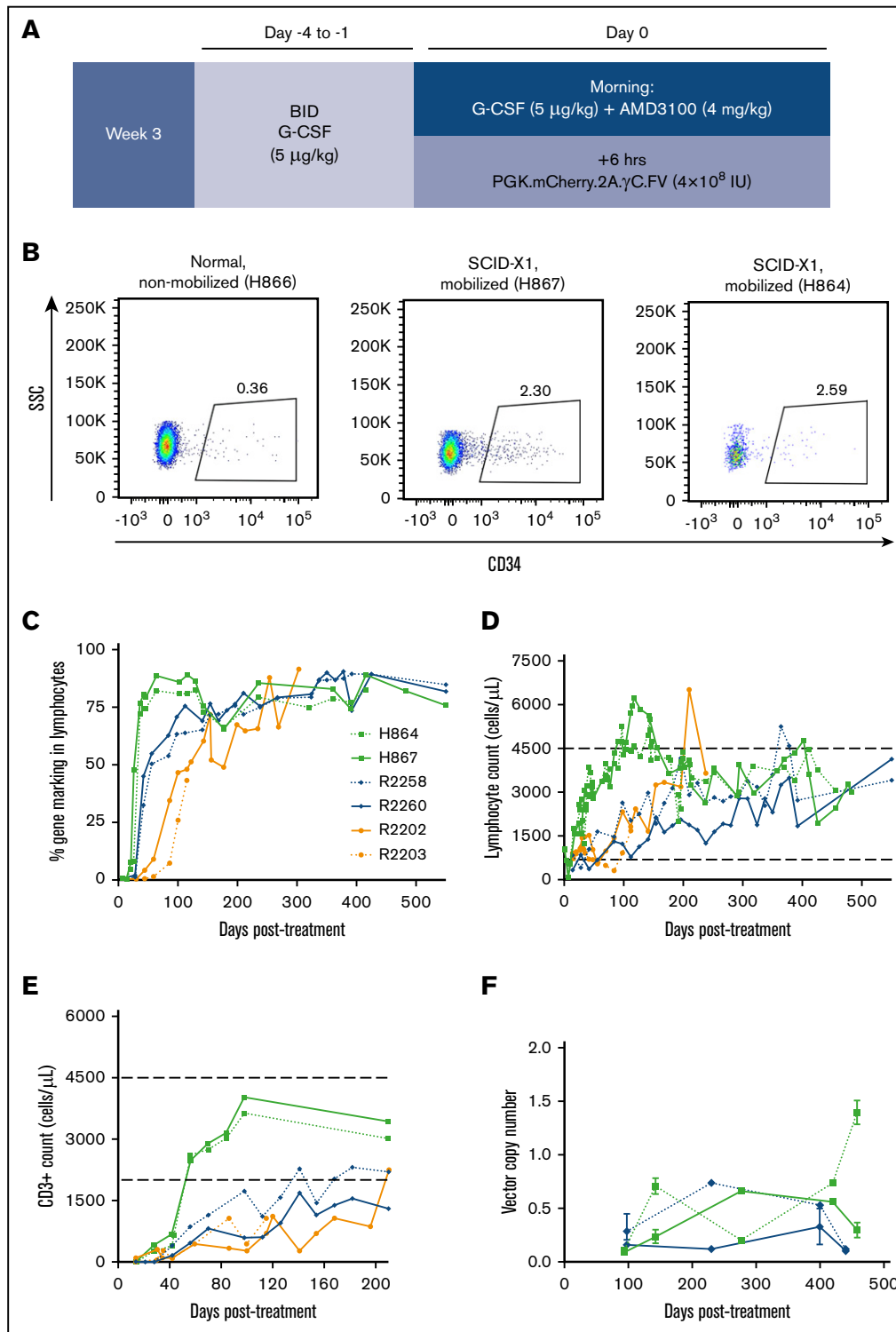


**Figure 2. Enhanced T-lymphocyte reconstitution with G-CSF/AMD3100 treatment before FV vector injection.** (A) Schematic of experiment involving G-CSF/AMD3100 treatment before FV vector injection. (B) Flow cytometry plot of peripheral blood CD34<sup>+</sup> cells in nonmobilized (H866) or mobilized (H867) newborn canines at 6 hours posttreatment. (C) Kinetics of gene marking based on fluorophore expression in circulating lymphocytes from dogs treated with different FV vectors with or without G-CSF/AMD3100 mobilization. Lymphocyte population was defined based on forward and side scatter (SSC). (D) Kinetics of lymphocyte reconstitution (lymphocytes per microliter of peripheral blood) in the same animals described in panel C. (E) Kinetics of CD3<sup>+</sup> cells reconstitution (cells per microliter of peripheral blood) in the same animals described in panel C during the first 7 months posttreatment. In panels D and E, normal range of lymphocyte/CD3<sup>+</sup> cell counts is shown by horizontal dashed lines. Animal R2203 only survived for 119 days posttreatment. (F) FV vector copy number measured longitudinally in peripheral blood leukocytes from unmobilized animals R2258/R2260 and mobilized animals H864/H867. BID, twice per day.

mobilized animals (Figure 2D); absolute CD3<sup>+</sup> lymphocyte counts reached  $2.5 \times 10^9/L$  in mobilized animals at 40 days post-FV vector injection as compared with  $\sim 0.1$  and  $0.4 \times 10^9/L$  in nonmobilized animals injected with EF1 $\alpha$ . $\gamma$ C.FV or competitively with PGK. $\gamma$ C.FV and EF1 $\alpha$ . $\gamma$ C.FV, respectively (compare H864/H867 with R2202/R2203 and R2258/R2260; Figure 2E). Vector copy number measured longitudinally from peripheral blood was comparable in mobilized and nonmobilized animals and steadily increased over a range of 0.1 to 1.5 (Figure 2F). We also verified that corrected lymphocytes expressed IL-2 receptor  $\gamma$ C by surface antibody staining and found slightly higher  $\gamma$ C expression in treated SCID-X1 animal H867 as compared with the normal littermate control H866 (supplemental Figure 2C). Despite substantially improving T-lymphocyte reconstitution, HSPC mobilization did not increase gene marking in myeloid cells or B lymphocytes. (supplemental Figure 3).

We hypothesized that in addition to improving kinetics of lymphocyte reconstitution, mobilization may also enhance clonal diversity of gene-corrected cells. RIS analysis from peripheral white blood cell DNA showed a marked increase in integration events (ie, clones) in mobilized dogs H864 and H867 as compared with nonmobilized dogs R2258 and R2260, despite use of an equal dose of PGK. $\gamma$ C.FV (Table 1). As shown in Figure 3 (legend in supplemental Figure 4), the fraction of clones that contributed to <1% of total gene marking (represented by gray area) was higher in the mobilized animals as compared with nonmobilized animals (<35% in R2258 and R2260 [Figure 3A] vs 75% to 85% in H864 and H867 [Figure 3B]). No clonal dominance was observed in any animal, but some persisting clones contributing to >10% of total gene marking were found in the nonmobilized animals, albeit with no indication of expansion (Figure 3A). Taken together, these data suggest that G-CSF/AMD3100 treatment before IV FV vector delivery increases both the kinetics of lymphocyte recovery and the diversity of immune reconstitution in SCID-X1 canines.

### Improved thymic output and broad TCR repertoire in mobilized FV-treated animals

Lymphocytes originating from the thymus that have not yet been exposed to antigens express a naive CD45RA<sup>+</sup> phenotype, thus providing a measure of thymic output. The 2 nonmobilized FV vector-treated animals (R2258 and R2260) initially showed normal frequency ( $\sim 90\%$ ) of CD3<sup>+</sup>CD45RA<sup>+</sup> T cells in peripheral blood, but their frequency subsequently declined to  $\sim 50\%$  at 1 year posttreatment (Figure 4A). In comparison, levels of CD3<sup>+</sup>CD45RA<sup>+</sup> cells remained stable in mobilized dogs H864 and H867 for at least 15 months posttreatment and continue to be monitored (Figure 4B). Thymic output was assessed independently by analysis of TRECs originating from TCR gene rearrangement during T-lymphocyte maturation. In the nonmobilized animals, TRECs were initially 10-fold lower in treated dogs, as compared with a normal littermate control, and then gradually declined over time (Figure 4C). In contrast, TRECs in the mobilized animals reached normal levels as early as 3 months posttreatment and remained similar to the littermate control up to  $\sim 400$  days posttreatment (Figure 4D). Despite a drop seen at later time points, TREC levels were maintained at higher levels in the mobilized animals relative to nonmobilized animals. In summary, mobilization before FV vector injection of SCID-X1 canines increased thymic output to levels comparable to those in a healthy control.

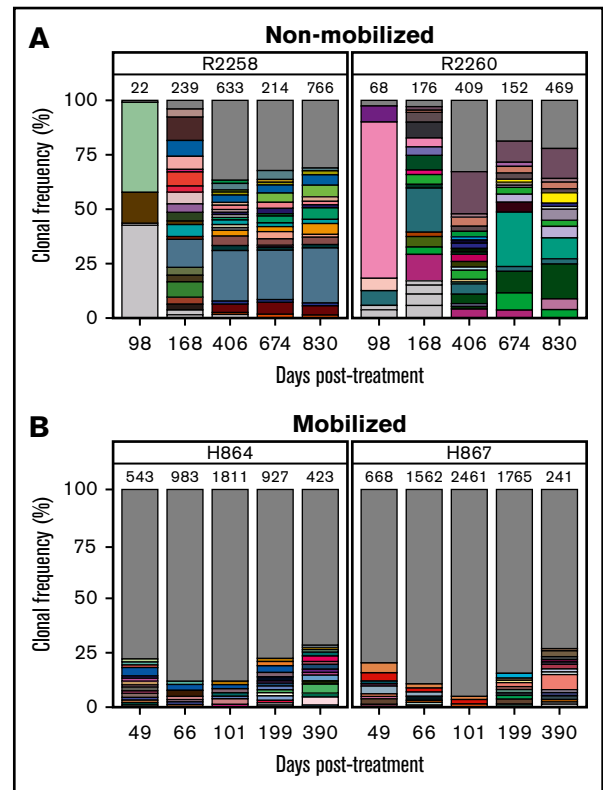


**Figure 3. Clonal diversity as determined by RIS analysis in nonmobilized and G-CSF/AMD3100-mobilized dogs before FV vector injection.** (A) Clonal diversity in nonmobilized canines R2258 (left) and R2260 (right) at the indicated time points posttreatment. (B) Clonal diversity in mobilized canines H864 (left) and H867 (right) at the indicated time points posttreatment with G-CSF/AMD3100 and vector PGK. $\gamma$ C.FV. In all graphs, unique RISs are plotted based on the number of times the RIS was sequenced and normalized to the percentage of total RISs captured at each time point for each animal. Total number of unique RISs is shown on top of each bar. Captured RISs appearing at a frequency >1% in each sample are represented by boxes in each graph. Boxes are colored in white if they were identified at a single time point or in matching colors if they were identified in >1 time point at a frequency >1%. The gray portion of the graph depicts all RISs with a frequency <1% at each time point. Legends describing the precise chromosomal location of RISs are given in supplemental Figure 4.

A majority of expanded CD3<sup>+</sup> lymphocytes were mature, expressing the coreceptor CD4 or CD8, with a small fraction of cells being CD4/CD8 double positive or double negative (supplemental Figure 5A-B). Both mobilized animals H864 and H867, as well as nonmobilized animal R2258, showed normal CD4:CD8 cell ratios, averaging 2, whereas nonmobilized animal R2260 showed an inverted ratio. The reason for this skewed ratio is not well understood but may have been caused by ongoing chronic infections, as observed in our previous study.<sup>30</sup> A majority of circulating T lymphocytes in R2258/R2260 and H864/H867 stained positive for TCR  $\alpha\beta$  starting at 2 months posttreatment, consistent with observations from healthy canines and humans (supplemental Figure 5C; data not shown). We assessed TCR diversity in each treated animal by TCR vector  $\beta$  spectratyping, which analyzes genetic rearrangement of the variable region of the TCR  $\beta$  gene. The 2 animals mobilized with G-CSF/AMD3100

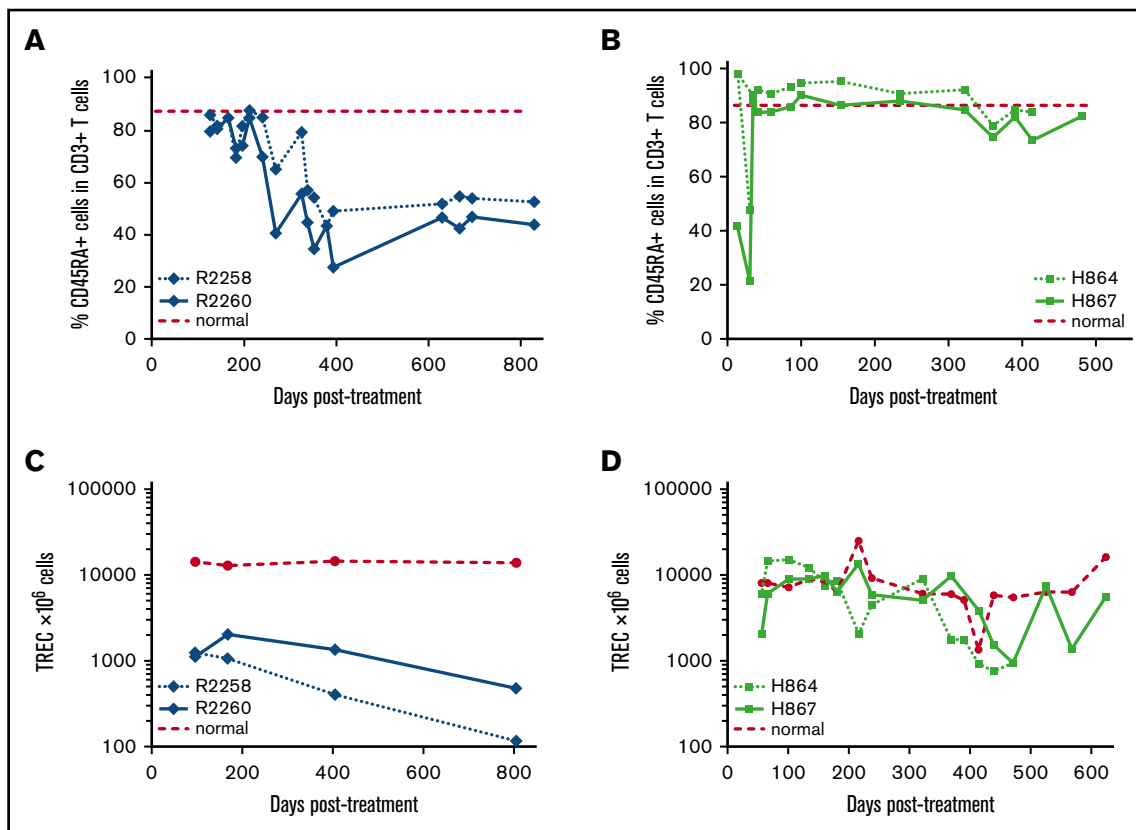


**Figure 4. Thymic output in FV vector-treated animals with and without G-CSF/AMD3100 mobilization.** (A) Fraction of CD45RA<sup>+</sup> cells within the CD3<sup>+</sup> population in peripheral blood of nonmobilized animals R2258 and R2260. (B) Fraction of CD3<sup>+</sup>CD45RA<sup>+</sup> cells in animals H864 and H867 treated with G-CSF/AMD3100 mobilization and vector PGK.γC.FV. (C) TREC levels in peripheral blood of the same animals shown in panel A. (D) TREC levels measured in the same animals shown in panel B. In panels A and B, dashed line shows average percentage of CD45RA<sup>+</sup> cells from normal dog; in panels C and D, dashed line shows TREC levels from a normal littermate control.

showed robust spectratype profiles, characterized by Gaussian distribution of fragments sized across 17 families of TCR vector β segments up to at least 1 year posttreatment, similar to that of an aged-matched normal littermate (Figure 5A-B). In comparison, the spectratype profile of nonmobilized animal R2258 seemed normal throughout the experiment, but the profile of R2260 was weaker, suggesting lower TCR diversity (supplemental Figure 6). Together, 3 of the 4 FV-treated SCID-X1 animals showed normal T-cell maturation and TCR diversity representative of healthy animals.

### Restoration of T- and B-lymphocyte function in PGK.γC.FV-treated animals

The functionality of the γC-dependent signaling pathways in corrected lymphocytes obtained from all FV-treated animals was verified by measuring tyrosine phosphorylation of the effector molecule STAT3 after in vitro stimulation with IL-21. As compared with cells obtained from a normal littermate control, equivalent levels of STAT3 phosphorylation were detected in CD3<sup>+</sup> lymphocytes from nonmobilized SCID-X1 dogs R2258 and R2260 (Figure 6A) or from mobilized FV-treated animals H864 and H867 (supplemental Figure 7). We further confirmed that T lymphocytes isolated from these animals could respond and proliferate when exposed to the T-cell mitogen phytohemagglutinin (Figure 6B). In conclusion, these results demonstrate restoration of T cell-specific signaling pathways in FV-treated SCID-X1 dogs.

Next, we evaluated primary and secondary antibody responses and immunoglobulin class switching after immunization with the T cell-dependent neoantigen bacteriophage φX174. All treated animals exhibited primary and secondary antibody responses that were within the range of those of normal canine control (compare blue and green lines with black line; Figure 7A), with no noticeable differences between mobilized and nonmobilized animals. Polyclonal IgM, IgG, and IgA concentrations were also measured from serum of mobilized dogs at 14 and 15 months posttreatment and showed a slight increase in IgM levels with a corresponding decrease in IgA in the treated SCID animals as compared with littermate control, indicating partial restoration of B-lymphocyte function (Figure 7B). The low levels of corrected peripheral B lymphocytes detected in these animals (ranging from 0% to 4%; supplemental Figures 2A and 3C) may account for this partial restoration of humoral responses.

### Safety of in vivo FV vector gene therapy and G-CSF/AMD3100 treatment

In vivo gene therapy proved beneficial for all SCID-X1 dogs; the nonmobilized animals (R2258 and R2260) lived for >2.5 years in a nonsterile environment, and the 2 mobilized animals (H864 and H867) are currently >16 months of age. Complete blood cell count analysis for all animals remained within the normal range

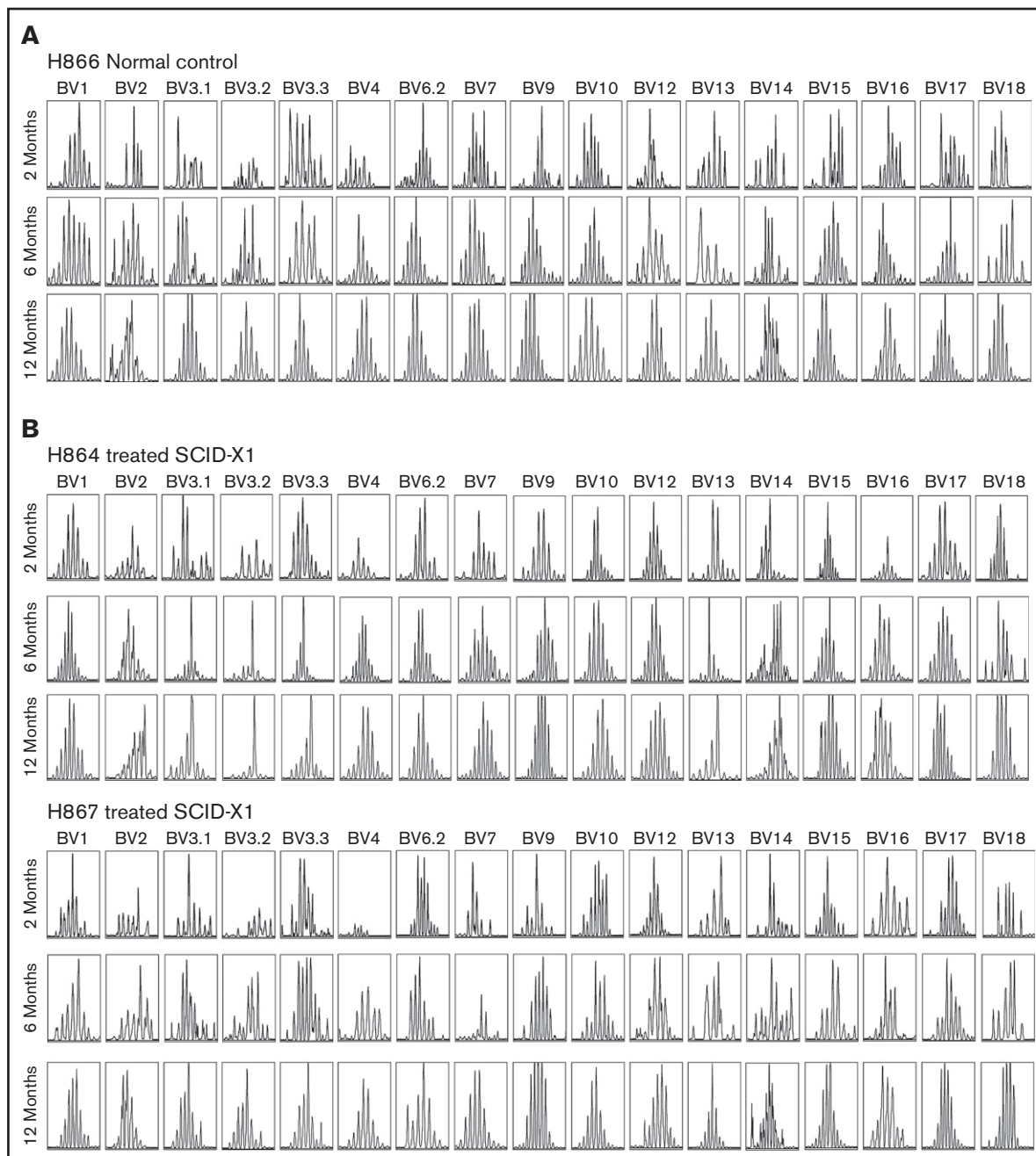


**Figure 5. TCR diversity as determined by TCR vector  $\beta$  spectratyping in mobilized FV vector-treated dogs.** Rearrangement of the TCR  $\beta$  chain was assessed by PCR amplification of complementary DNA using 17 different primer pairs (annotated on top) at various time points posttreatment in a normal littermate control H866 (A) and in treated SCID-X1 dogs H864 and H867 (B).

during the first year posttreatment, but neutrophil and monocyte counts gradually increased at later time points (supplemental Figure 8A-E), probably reflecting inflammatory responses to parasitic or viral infection. R2258 and R2260 eventually developed papillomavirus (PV) infections, similar to observations from SCID-X1 canines<sup>43</sup> or patients treated with BMT or gene therapy,<sup>4,44</sup> and had to be euthanized at 830 days posttreatment. Tissues from these animals were collected and analyzed by RIS for biodistribution assessment of the foamy provirus. A vast majority of RISs (>90%) detected in tissues (supplemental Figure 9) were also found in

peripheral blood samples at the same time point, indicating that they originated from contaminating blood cells present in perfused tissues (supplemental Figure 10). Ovaries and testes showed the smallest number of integration events (37 and 56, respectively, as compared with 766 and 469 in blood), and none of the RISs found exclusively in the gonad tissues (ie, unique RIS) appeared at biologically relevant frequencies, except for 1 integration site in the ovaries (chromosome 38; 34 522; 4.28%; supplemental Table 1A). No unique RIS at a biologically relevant frequency was detected in semen from male H867



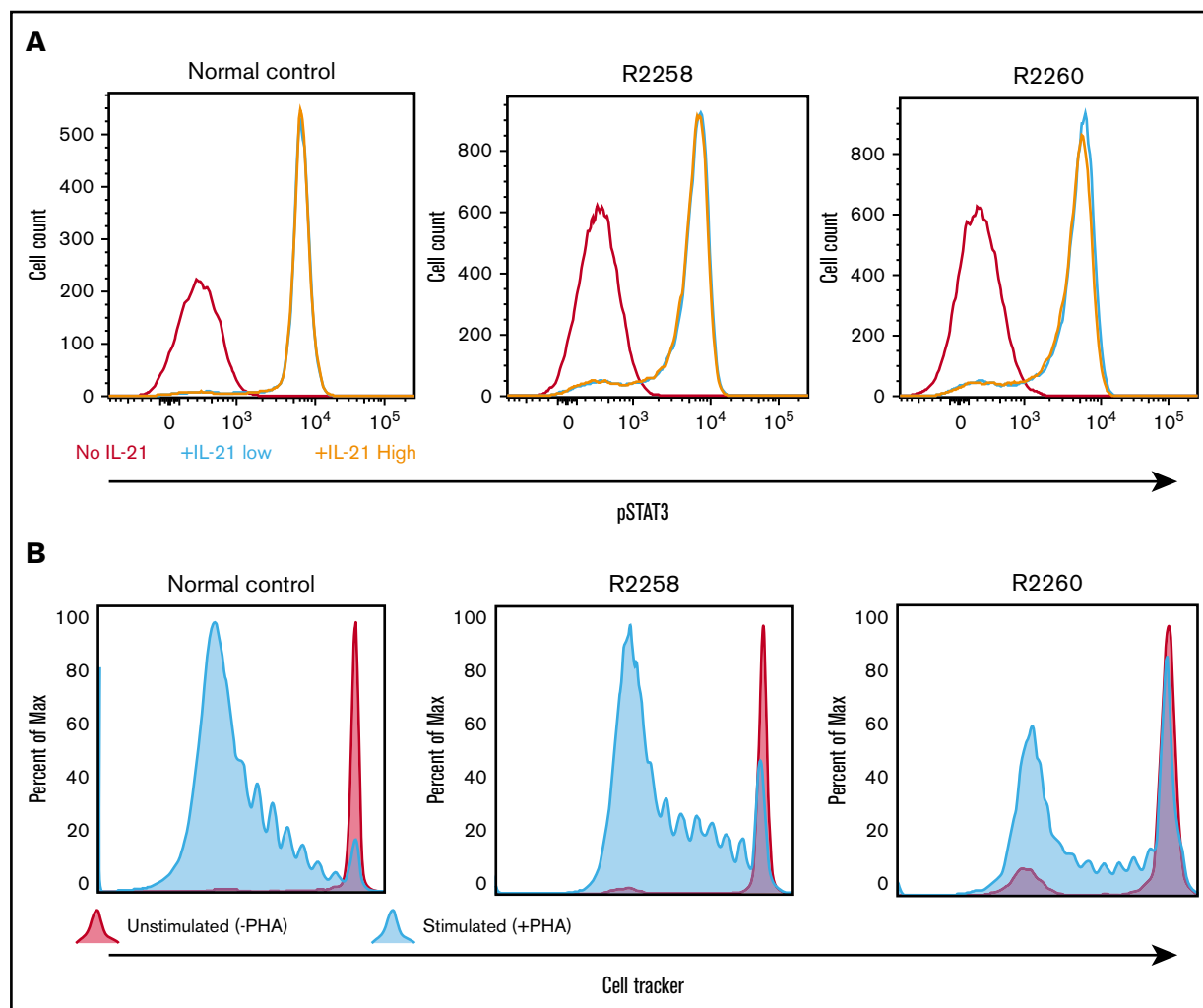


**Figure 6. Validation of T-lymphocyte function in cells obtained from FV vector-treated SCID-X1 canines.** (A) pSTAT3 was measured in PBMCs isolated from animals R2258 and R2260 (nonmobilized; 485 days posttreatment) or from a normal littermate control and cultured *in vitro* with no, low, or high levels of IL-21. pSTAT3 signal is gated from CD3<sup>+</sup> cells. (B) Proliferative response to phytohemagglutinin of PBMCs isolated from the same animals and same time point shown in panel A. Cell proliferation was determined by dilution of CellTracker dye.

(supplemental Figure 11; supplemental Table 1B). Taken together, these results suggest that off-target transduction events by *in vivo* FV vector treatment are rare events, with no compelling evidence of provirus integration in the germ line, a finding also supported by the study of progeny issued from FV-treated male R2260, discussed in the next section (supplemental Table 2).

## Discussion

*Ex vivo* HSC gene therapy clinical trials involving SCID-X1 patients are demonstrating clear clinical benefits (reviewed by Cavazzana et al<sup>45</sup>) but require elaborate protocols, sophisticated facilities, and genotoxic conditioning. Here, we propose a simpler, safer, and more versatile gene therapy approach to SCID-X1 that involves the direct IV injection of FV vectors with no prior conditioning regimen. Important improvements in our method were made by mobilizing HSPCs with G-CSF and AMD3100 before injection with an optimized FV vector containing a stronger enhancerless PGK

promoter. Kinetics of lymphocyte reconstitution were markedly increased, presumably because of transduction of a greater pool of lymphocyte precursors in blood, which also enhanced thymopoiesis and clonal diversity. As compared to our previous study where all EF1 $\alpha$ - $\gamma$ C.FV-treated animals succumbed to chronic infections by 330 days posttreatment,<sup>30</sup> survival was improved in all PGK- $\gamma$ C.FV-treated SCID-X1 dogs, which lived for as long as 2.5 years.

A critical parameter in vector design is the choice of a promoter-enhancer element with sufficient strength to drive efficient immune reconstitution and with minimal risk of inadvertent enhancer-mediated gene transactivation. All current SCID-X1 clinical trials use viral vectors containing the EF1 $\alpha$  promoter to drive expression of the  $\gamma$ C gene.<sup>3,4</sup> This choice of promoter was validated in previous studies that compared genotoxic risks associated with the physiological cellular promoters from the human EF1 $\alpha$  or PGK genes or from the endogenous  $\gamma$ C gene.<sup>46,47</sup> In addition, in a murine model of SCID-X1, progenitor cells transduced with the EF1 $\alpha$ -containing LV completely restored lymphoid development

and immune function, whereas cells modified with PGK-containing vector resulted in poor immune reconstitution.<sup>48</sup> Nevertheless, the long form (~1200 bp) of EF1 $\alpha$  promoter was used in this study, whereas our EF1 $\alpha$ . $\gamma$ C.FV vector contains the shorter form (~250 bp), similar to the clinically approved vector.<sup>4</sup> Our competitive injections of EF1 $\alpha$ . $\gamma$ C.FV and PGK. $\gamma$ C.FV vectors of SCID-X1 pups clearly showed superiority of the PGK vector, which accounted for >80% of gene marking, and no evidence of clonal dominance. Superior performance of the PGK promoter was similarly demonstrated in a radiation-sensitive SCID murine model with complete functional correction of the Artemis gene achieved with a PGK LV, whereas cytomegalovirus LV or EF1 $\alpha$  LV led to incomplete correction<sup>49</sup>; efficacy of a PGK. $\gamma$ C SIN LV was also validated for ex vivo SCID-X1 gene therapy using a murine model.<sup>50</sup> Although it remains to be determined whether the PGK promoter is a better choice in other delivery methods and disease contexts, stronger expression of the  $\gamma$ C transgene, as determined by the fluorescence reporter, correlated with increased vector performance in our model.

G-CSF and AMD3100 in combination have been used successfully to increase CD34<sup>+</sup> cells in peripheral blood of mice, nonhuman primates, and humans.<sup>39,40,42</sup> Both G-CSF and AMD3100 have mobilizing properties by acting on distinct cellular pathways, and combinatory treatment has resulted in additive effects.<sup>51</sup> G-CSF suppresses osteoblast lineage cells in the bone marrow niche, leading to reduced levels of signaling molecules (eg, CXCL12, VLA-4, c-Kit), which are essential for HSPC retention.<sup>52</sup> The bicyclam AMD3100 is a potent, selective, and reversible antagonist of the CXCR4 chemokine receptor that disrupts the binding of CXCR4 to SDF-1, thereby mobilizing HSCs into the blood.<sup>41,53</sup> Kinetics of HSPC mobilization by AMD3100 alone were previously assessed in adult dogs,<sup>54</sup> in which the treatment was well tolerated and circulating CD34<sup>+</sup> cells increased three- to 10-fold, with peak mobilization at 8 to 10 hours posttreatment. Similarly, G-CSF/AMD3100 mobilization of immunodeficient humanized mice increased colony forming units isolated from peripheral blood by 2.3- and 8.2-fold, respectively.<sup>42</sup> Our mobilization of SCID-X1 pups with G-CSF/AMD3100 showed a comparable sevenfold increase in circulating CD34<sup>+</sup> cells at 6 hours posttreatment.

Beyond mobilizing HSPCs in peripheral blood, G-CSF and AMD3100 also affect other cell lineages. Circulating lymphocyte and monocyte counts were increased by medians of 1.5- and fourfold, respectively, in mobilized adult canines as compared with untreated controls.<sup>54</sup> In rhesus macaques, AMD3100 increased numbers of B and T lymphocytes, which included CD4<sup>+</sup> and CD8<sup>+</sup> T cells, central and effector memory T cells, and NK cells in peripheral blood.<sup>55</sup> In addition, macaques receiving transplants of G-CSF/AMD3100-mobilized CD34<sup>+</sup> cells manifested faster lymphocyte recovery as compared with nonmobilized animals, likely because of increased blood count of lymphoid precursors.<sup>56</sup> Our demonstration of faster blood T-lymphocyte recovery and increased thymopoiesis and clonal diversity in G-CSF/AMD3100-mobilized SCID-X1 pups implies that a larger pool of T-cell progenitors was transduced after IV-delivered FV vectors. These corrected T-cell progenitors may directly home to the thymus, as suggested by previous findings,<sup>57</sup> and subsequently mature into CD4<sup>+</sup> and/or CD8<sup>+</sup> T lymphocytes. The decline in both TRECs and CD45RA<sup>+</sup> na $\ddot{u}$ ve T cells at 8 to 9 months posttreatment in the 2 nonmobilized canines can be explained either by the inability of the hypoplastic SCID thymus to sustain

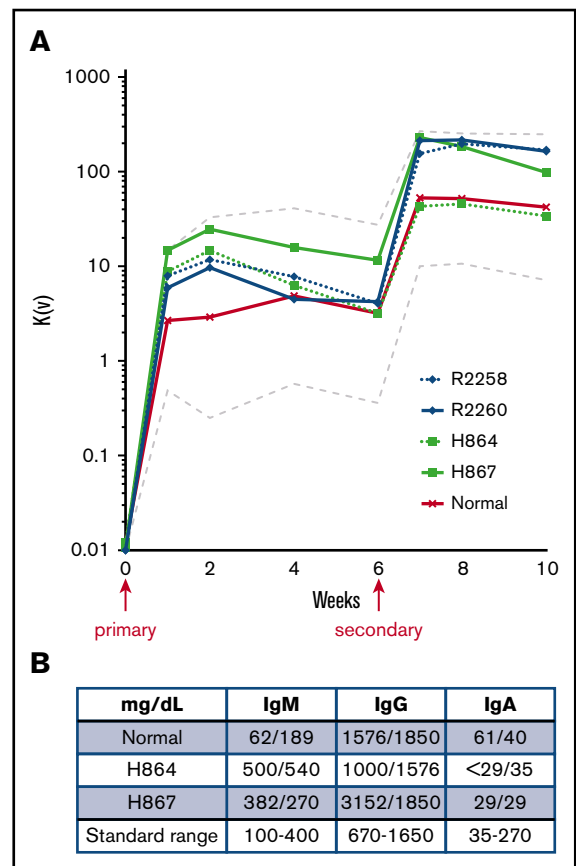


**Figure 7. Immunoglobulin responses in treated SCID-X1 canines. (A)** Bacteriophage immunoglobulin response in serum of FV-treated SCID-X1 dogs (mobilized, green; nonmobilized, blue) and in a normal control (red)  $\pm$  2 standard deviations (dashed lines). Animals were injected with a first dose of bacteriophage  $\phi$ X174 at 8 to 12 months post-FV vector treatment and with a second dose 6 weeks later. Primary and secondary immune responses to injection were assessed at 1, 2, and 4 weeks, compared with preinjection levels, and expressed as the rate of phage inactivation or K value (Kv; described in Methods). (B) Quantitative measurement of the 3 main classes of immunoglobulin in serum of mobilized animals at 14 and 15 months posttreatment as compared with a normal control. Standard range is based on normal dog age 1 year.

thymopoiesis or by the poor engraftment of gene-corrected HSCs capable of self-renewal and continuous production of functional T cells. G-CSF/AMD3100 mobilization substantially increased TREC levels in treated SCID-X1 animals and may help prolong thymic output.

The 2 nonmobilized FV-treated animals developed cutaneous warts because of severe PV disease at ~28 months posttreatment after arrival in the new canine colony. Both SCID-X1 canines and human patients are known to be susceptible to PV infections.<sup>43,44</sup> A retrospective study of 41 SCID human patients who survived >10 years after BMT reported that 50% of patients developed chronic severe PV infection.<sup>44</sup> No correlation could be drawn between PV disease and NK count or function, despite the capacity of NK cells to eliminate PV-infected cells. Deficiency in function of keratinocytes, the target cells of PV infection, provides an alternative explanation for PV susceptibility, because they express  $\gamma$ C-dependent cytokine receptors such as IL-4, which activates the

release of proinflammatory cytokines under normal conditions. Further work is needed to better define the function of  $\gamma$ C-dependent signaling pathway in anti-human PV immunity.

Upon sexual maturity, treated male R2260 sired 3 litters via artificial insemination, overall resulting in a normal pedigree and arguing against possible transduction of the germ line by FV vectors, thus corroborating our RIS data showing absence of relevant integration site in semen obtained from H867. Although 1 unique integration site was documented in ovaries from R2258, it may have originated from transduction of accessory cells and not from germ cells.

BMT has traditionally been the preferred treatment of SCID-X1 patients, but recent findings have demonstrated faster T-cell reconstitution in SCID-X1 patients treated by ex vivo gene therapy as compared with haploidentical HSC transplantation,<sup>3,4,58,59</sup> suggesting that gene therapy may ultimately become the front-line therapeutic modality. With the caveat of comparing different species and age groups, we find that our improved conditions using G-CSF/AMD3100 mobilization before FV vector injection result in comparable or higher CD3<sup>+</sup> cell reconstitution in treated SCID-X1 pups as compared with SCID-X1 patients treated with ex vivo SIN RV or SIN LV gene therapy.<sup>3,4,59</sup> Of note, data from SCID-X1<sup>4</sup> and adenosine deaminase SCID patients<sup>60</sup> indicate that low-dose conditioning with busulfan is well tolerated in patients undergoing retroviral-based gene therapy and is emerging as standard of care for the treatment of these primary immunodeficiencies.

Overall, our study demonstrates the safety, feasibility, and efficacy of FV vectors for in vivo gene therapy and suggests that this approach may provide prompt and effective treatment of newborn SCID-X1 patients in the future after routine genetic screening without the complications associated with ex vivo manipulation of HSCs or conditioning. Beyond SCID-X1, this methodology may be applicable in patients with Fanconi anemia, who have a genetic defect in DNA crosslink repair, where functionally corrected cells have a natural selective advantage, and transduction of the therapeutic gene into a few stem cells is expected to be sufficient

for therapeutic efficacy. Ex vivo gene therapy in patients with Fanconi anemia currently presents important challenges because of the low number and fragility of CD34<sup>+</sup> HSPCs recovered from bone marrow or mobilized peripheral blood.<sup>61</sup> In vivo gene therapy thus offers an interesting alternative approach, and future work will focus on the redesigning of the viral vector to exclusively target primitive HSCs.

## Acknowledgments

The authors thank the veterinary staff at the Fred Hutchinson Cancer Research Center and University of Pennsylvania, Ray Carrillo for technical assistance, Lauren Scheffer for her assistance with the retrovirus integration site analysis, Helen Crawford and Bonnie Larson for their help with manuscript and figure preparations, and Ted Gooley and Philip Stevenson for their help with statistical analysis.

This work was supported in part by National Institutes of Health, National Institute of Allergy and Infectious Diseases grant 5P01AI097100-05 (H.-P.K., G.D.T., J.E.A., A.M.S., P.J.F., and D.J.R.) and National Heart, Lung, and Blood Institute grant HL122173 (H.-P.K.).

## Authorship

Contribution: H.-P.K., G.D.T., A.M.S., P.J.F., and D.J.R. conceived the project and designed the experiments; O.H., F.C., Y.S.R., J.E.A., and C.R.B. designed and performed experiments; N.W.H., D.H., and P.O. performed experiments; Z.K.N. performed all bioinformatic analyses and generated all retrovirus integration site figures; O.H. wrote the paper; H.-P.K., D.J.R., T.R.T., F.C., Y.S.R., and Z.K.N. edited the manuscript; and F.C. and O.H. assembled the figures.

Conflict-of-interest disclosure: The authors declare no competing financial interests.

Correspondence: Hans-Peter Kiem, Fred Hutchinson Cancer Research Center, 1100 Fairview Ave N., D1-100, Seattle, WA 98109-1024; e-mail: hkiem@fredhutch.org.

## References

1. Buckley RH, Schiff SE, Schiff RI, et al. Hematopoietic stem-cell transplantation for the treatment of severe combined immunodeficiency. *N Engl J Med*. 1999;340(7):508-516.
2. Pai SY, Logan BR, Griffith LM, et al. Transplantation outcomes for severe combined immunodeficiency, 2000-2009. *N Engl J Med*. 2014;371(5):434-446.
3. Hacein-Bey-Abina S, Pai SY, Gaspar HB, et al. A modified  $\gamma$ -retrovirus vector for X-linked severe combined immunodeficiency. *N Engl J Med*. 2014;371(15):1407-1417.
4. De Ravin SS, Wu X, Moir S, et al. Lentiviral hematopoietic stem cell gene therapy for X-linked severe combined immunodeficiency. *Sci Transl Med*. 2016;8(335):335ra57.
5. Noguchi M, Nakamura Y, Russell SM, et al. Interleukin-2 receptor gamma chain: a functional component of the interleukin-7 receptor. *Science*. 1993;262(5141):1877-1880.
6. Henthorn PS, Somberg RL, Fimiani VM, Puck JM, Patterson DF, Felsburg PJ. IL-2R gamma gene microdeletion demonstrates that canine X-linked severe combined immunodeficiency is a homologue of the human disease. *Genomics*. 1994;23(1):69-74.
7. Leonard WJ. Dysfunctional cytokine receptor signaling in severe combined immunodeficiency. *J Invest Med*. 1996;44(6):304-311.
8. Conley ME, Buckley RH, Hong R, et al. X-linked severe combined immunodeficiency. Diagnosis in males with sporadic severe combined immunodeficiency and clarification of clinical findings. *J Clin Invest*. 1990;85(5):1548-1554.
9. Gougeon ML, Dreon G, Le Deist F, et al. Human severe combined immunodeficiency disease: phenotypic and functional characteristics of peripheral B lymphocytes. *J Immunol*. 1990;145(9):2873-2879.

10. Gendelman HE, Ehrlich GD, Baca LM, et al. The inability of human immunodeficiency virus to infect chimpanzee monocytes can be overcome by serial viral passage in vivo. *J Virol*. 1991;65(7):3853-3863.
11. Buckley RH, Schiff SE, Schiff RI, et al. Haploidentical bone marrow stem cell transplantation in human severe combined immunodeficiency. *Semin Hematol*. 1993;30(4 suppl 4):92-101, discussion 102-104.
12. Matthews DJ, Clark PA, Herbert J, et al. Function of the interleukin-2 (IL-2) receptor gamma-chain in biologic responses of X-linked severe combined immunodeficient B cells to IL-2, IL-4, IL-13, and IL-15. *Blood*. 1995;85(1):38-42.
13. Rosen A, Lundman P, Carlsson M, et al. A CD4+ T cell line-secreted factor, growth promoting for normal and leukemic B cells, identified as thioredoxin. *Int Immunol*. 1995;7(4):625-633.
14. Felsburg PJ, De Ravin SS, Malech HL, Sorrentino BP, Burtner C, Kiem HP. Gene therapy studies in a canine model of X-linked severe combined immunodeficiency. *Hum Gene Ther Clin Dev*. 2015;26(1):50-56.
15. Ting-De Ravin SS, Kennedy DR, Naumann N, et al. Correction of canine X-linked severe combined immunodeficiency by in vivo retroviral gene therapy. *Blood*. 2006;107(8):3091-3097.
16. Hooks JJ, Gibbs CJ Jr. The foamy viruses [review]. *Bacteriol Rev*. 1975;39(3):169-185.
17. Falcone V, Schweizer M, Neumann-Haefelin D. Replication of primate foamy viruses in natural and experimental hosts [review]. *Curr Top Microbiol Immunol*. 2003;277:161-180.
18. Flügel RM. Spumaviruses: a group of complex retroviruses [review]. *J Acquir Immune Defic Syndr*. 1991;4(8):739-750.
19. Vassilopoulos G, Trobridge G, Josephson NC, Russell DW. Gene transfer into murine hematopoietic stem cells with helper-free foamy virus vectors. *Blood*. 2001;98(3):604-609.
20. Josephson NC, Vassilopoulos G, Trobridge GD, et al. Transduction of human NOD/SCID-repopulating cells with both lymphoid and myeloid potential by foamy virus vectors. *Proc Natl Acad Sci USA*. 2002;99(12):8295-8300.
21. Kiem HP, Allen J, Trobridge G, et al. Foamy-virus-mediated gene transfer to canine repopulating cells. *Blood*. 2007;109(1):65-70.
22. Trobridge GD, Allen J, Peterson L, Ironside C, Russell DW, Kiem HP. Foamy and lentiviral vectors transduce canine long-term repopulating cells at similar efficiency. *Hum Gene Ther*. 2009;20(5):519-523.
23. Trobridge GD, Miller DG, Jacobs MA, et al. Foamy virus vector integration sites in normal human cells. *Proc Natl Acad Sci USA*. 2006;103(5):1498-1503.
24. Hendrie PC, Huo Y, Stolitenko RB, Russell DW. A rapid and quantitative assay for measuring neighboring gene activation by vector proviruses. *Mol Ther*. 2008;16(3):534-540.
25. Bauer TR Jr, Allen JM, Hai M, et al. Successful treatment of canine leukocyte adhesion deficiency by foamy virus vectors. *Nat Med*. 2008;14(1):93-97.
26. Beard BC, Keyser KA, Trobridge GD, et al. Unique integration profiles in a canine model of long-term repopulating cells transduced with gammaretrovirus, lentivirus, or foamy virus. *Hum Gene Ther*. 2007;18(5):423-434.
27. Everson EM, Olzsko ME, Leap DJ, Hocum JD, Trobridge GD. A comparison of foamy and lentiviral vector genotoxicity in SCID-repopulating cells shows foamy vectors are less prone to clonal dominance. *Mol Ther Methods Clin Dev*. 2016;3:16048.
28. Olzsko ME, Adair JE, Linde I, et al. Foamy viral vector integration sites in SCID-repopulating cells after MGMTP140K-mediated in vivo selection. *Gene Ther*. 2015;22(7):591-595.
29. Josephson NC, Trobridge G, Russell DW. Transduction of long-term and mobilized peripheral blood-derived NOD/SCID repopulating cells by foamy virus vectors. *Hum Gene Ther*. 2004;15(1):87-92.
30. Burtner CR, Beard BC, Kennedy DR, et al. Intravenous injection of a foamy virus vector to correct canine SCID-X1. *Blood*. 2014;123(23):3578-3584.
31. Thakar MS, Santos EB, Fricker S, Bridger G, Storb R, Sandmaier BM. Plerixafor-mobilized stem cells alone are capable of inducing early engraftment across the MHC-haploidentical canine barrier. *Blood*. 2010;115(4):916-917.
32. Kiem HP, Wu RA, Sun G, von Laer D, Rossi JJ, Trobridge GD. Foamy combinatorial anti-HIV vectors with MGMTP140K potentially inhibit HIV-1 and SHIV replication and mediate selection in vivo. *Gene Ther*. 2010;17(1):37-49.
33. Adair JE, Beard BC, Trobridge GD, et al. Extended survival of glioblastoma patients after chemoprotective HSC gene therapy. *Sci Transl Med*. 2012;4(133):133ra57.
34. Adair JE, Johnston SK, Mrugala MM, et al. Gene therapy enhances chemotherapy tolerance and efficacy in glioblastoma patients. *J Clin Invest*. 2014;124(9):4082-4092.
35. Ochs HD, Davis SD, Wedgwood RJ. Immunologic responses to bacteriophage phi-X 174 in immunodeficiency diseases. *J Clin Invest*. 1971;50(12):2559-2568.
36. Wedgwood RJ, Ochs HD, Davis SD. Immunodeficiency in man and animals. In: Bergsma D, ed. The Recognition and Classification of Immunodeficiency Diseases with Bacteriophage ΦX174 March of Dimes Birth Defects Original Article Series X1. Sunderland, MA: Sinaur; 1975:331-338
37. Vernau W, Hartnett BJ, Kennedy DR, et al. T cell repertoire development in XSCID dogs following nonconditioned allogeneic bone marrow transplantation. *Biol Blood Marrow Transplant*. 2007;13(9):1005-1015.
38. Kennedy DR, Hartnett BJ, Kennedy JS, et al. Ex vivo  $\gamma$ -retroviral gene therapy of dogs with X-linked severe combined immunodeficiency and the development of a thymic T cell lymphoma. *Vet Immunol Immunopathol*. 2011;142(1-2):36-48.
39. Broxmeyer HE, Orschell CM, Clapp DW, et al. Rapid mobilization of murine and human hematopoietic stem and progenitor cells with AMD3100, a CXCR4 antagonist. *J Exp Med*. 2005;201(8):1307-1318.



40. Larochelle A, Krouse A, Metzger M, et al. AMD3100 mobilizes hematopoietic stem cells with long-term repopulating capacity in nonhuman primates. *Blood*. 2006;107(9):3772-3778.
41. Dar A, Schajnovitz A, Lapid K, et al. Rapid mobilization of hematopoietic progenitors by AMD3100 and catecholamines is mediated by CXCR4-dependent SDF-1 release from bone marrow stromal cells [published correction appears in *Leukemia*. 2011;25(8):1378]. *Leukemia*. 2011;25(8):1286-1296.
42. Richter M, Saydaminova K, Yumul R, et al. In vivo transduction of primitive mobilized hematopoietic stem cells after intravenous injection of integrating adenovirus vectors. *Blood*. 2016;128(18):2206-2217.
43. Goldschmidt MH, Kennedy JS, Kennedy DR, et al. Severe papillomavirus infection progressing to metastatic squamous cell carcinoma in bone marrow-transplanted X-linked SCID dogs. *J Virol*. 2006;80(13):6621-6628.
44. Laffort C, Le Deist F, Favre M, et al. Severe cutaneous papillomavirus disease after haemopoietic stem-cell transplantation in patients with severe combined immune deficiency caused by common gamma cytokine receptor subunit or JAK-3 deficiency. *Lancet*. 2004;363(9426):2051-2054.
45. Cavazzana M, Six E, Lagresle-Peyrou C, André-Schmutz I, Hacein-Bey-Abina S. Gene therapy for X-linked severe combined immunodeficiency: where do we stand? *Hum Gene Ther*. 2016;27(2):108-116.
46. Zychlinski D, Schambach A, Modlich U, et al. Physiological promoters reduce the genotoxic risk of integrating gene vectors. *Mol Ther*. 2008;16(4):718-725.
47. Zhou S, Mody D, DeRavin SS, et al. A self-inactivating lentiviral vector for SCID-X1 gene therapy that does not activate LMO2 expression in human T cells. *Blood*. 2010;116(6):900-908.
48. Ginn SL, Liao SH, Dane AP, et al. Lymphomagenesis in SCID-X1 mice following lentivirus-mediated phenotype correction independent of insertional mutagenesis and gamma overexpression. *Mol Ther*. 2010;18(5):965-976.
49. Mostoslavsky G, Fabian AJ, Rooney S, Alt FW, Mulligan RC. Complete correction of murine Artemis immunodeficiency by lentiviral vector-mediated gene transfer. *Proc Natl Acad Sci USA*. 2006;103(44):16406-16411.
50. Huston MW, van Til NP, Visser TP, et al. Correction of murine SCID-X1 by lentiviral gene therapy using a codon-optimized IL2RG gene and minimal pretransplant conditioning. *Mol Ther*. 2011;19(10):1867-1877.
51. Liles WC, Broxmeyer HE, Rodger E, et al. Mobilization of hematopoietic progenitor cells in healthy volunteers by AMD3100, a CXCR4 antagonist. *Blood*. 2003;102(8):2728-2730.
52. Winkler IG, Pettit AR, Raggatt LJ, et al. Hematopoietic stem cell mobilizing agents G-CSF, cyclophosphamide or AMD3100 have distinct mechanisms of action on bone marrow HSC niches and bone formation. *Leukemia*. 2012;26(7):1594-1601.
53. Rosenkilde MM, Gerlach LO, Jakobsen JS, Skerlj RT, Bridger GJ, Schwartz TW. Molecular mechanism of AMD3100 antagonism in the CXCR4 receptor: transfer of binding site to the CXCR3 receptor. *J Biol Chem*. 2004;279(4):3033-3041.
54. Burroughs L, Mielcarek M, Little MT, et al. Durable engraftment of AMD3100-mobilized autologous and allogeneic peripheral-blood mononuclear cells in a canine transplantation model. *Blood*. 2005;106(12):4002-4008.
55. Kean LS, Sen S, Onabajo O, et al. Significant mobilization of both conventional and regulatory T cells with AMD3100. *Blood*. 2011;118(25):6580-6590.
56. Uchida N, Bonifacino A, Krouse AE, et al. Accelerated lymphocyte reconstitution and long-term recovery after transplantation of lentiviral-transduced rhesus CD34+ cells mobilized by G-CSF and plerixafor. *Exp Hematol*. 2011;39(7):795-805.
57. Weerkamp F, Baert MR, Brugman MH, et al. Human thymus contains multipotent progenitors with T/B lymphoid, myeloid, and erythroid lineage potential. *Blood*. 2006;107(8):3131-3137.
58. Touzot F, Moshous D, Creidy R, et al. Faster T-cell development following gene therapy compared with haploidentical HSCT in the treatment of SCID-X1. *Blood*. 2015;125(23):3563-3569.
59. Mamcarz E, Zhou S, Lockey T, et al. Interim results from a phase I/II clinical gene therapy study for newly diagnosed infants with X-linked severe combined immunodeficiency using a safety-modified lentiviral vector and targeted reduced exposure to busulfan [abstract]. *Blood*. 2017;130(suppl 1). Abstract 523.
60. Cicalese MP, Ferrua F, Castagnaro L, et al. Update on the safety and efficacy of retroviral gene therapy for immunodeficiency due to adenosine deaminase deficiency. *Blood*. 2016;128(1):45-54.
61. Adair JE, Sevilla J, Heredia CD, Becker PS, Kiem HP, Bueren J. Lessons learned from two decades of clinical trial experience in gene therapy for Fanconi anemia. *Curr Gene Ther*. 2017;16(5):338-348.